Anti-Counterfeit Protection of Pharmaceutical Products with Spatial Mapping of X-Ray Detectable Barcodes and Logos

Daniele Musumeci, Chunhua Hu, Michael D. Ward*

Contribution from the Molecular Design Institute, Department of Chemistry, New York University, 100 Washington Square East, New York, NY 10003

Electronic Supporting Information

Table of Contents

Materials. Rutile, anatase and zinc oxide (Sigma-Aldrich, St. Louis, MO, USA) were purchased and used as obtained without further purification (see Supporting Information). Light corn syrup was purchased from ACH Food Companies Inc. (Memphis, TN, USA). Coated 325 mg aspirin tablets were purchased from CVS Pharmacy Inc. (Woonsocket, RI, USA). Coated 200 mg ibuprofen tablets were purchased from DuaneReade (New York, NY, USA). Glistening metallic spray paint was purchased from Krylon Products Group (Cleveland, OH, USA). Sylgard® 184 Poly dimethyl siloxane (PDMS) and Sylgard® 184 silicone elastomer curing agent were purchased from Dow Corning Corporation (Midland, MI, USA). Glass microscope slides were purchased from Fisher Scientific (Pittsburgh, PA, USA). Silicon wafers (100) were purchased from Universitywafer (South Boston, MA, USA). Polyethylene film was purchased from The Glad Products Company (Oakland, CA, USA). Plastic masks for photolithography were obtained from CAD Art Services Inc. (Bandon, OR, USA).

Stamp fabrication. PDMS elastomer stamps were fabricated using conventional methods. A layer of SU-8 negative photoresist was spin-coated onto silicon wafers and exposed to UV light (365 nm) for 45 seconds through a plastic mask with transparent features corresponding to the desired stamp master. The removal of the unexposed non-polymerized photoresist was performed by dipping the silicon wafer into a 1-methoxy-2-propyl acetate developing solution for six minutes, thereby producing the desired stamp master features on the wafer surface. PDMS stamps were prepared using these silicon surfaces as master molds. PDMS was first thoroughly mixed with the curing agent (at a 10:1 w/w ratio) and allowed to stand under vacuum for 30 minutes at room temperature to allow escape of air bubbles from the mixture. The stamp was then fabricated by pouring the mixed elastomer into the silicon master mold, cured in an oven at

120 ºC for 5 hours, and peeled from the master mold, thereby producing a negative pattern of the master.

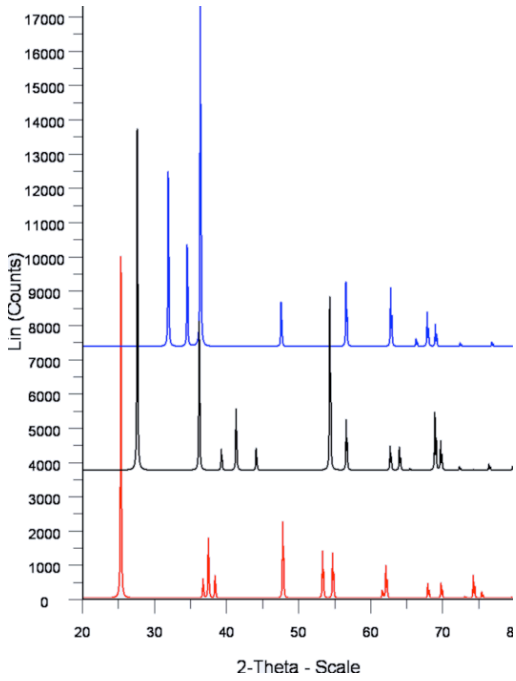

Figure S-1. X-ray powder diffraction patterns of anatase (red), rutile (black) and zinc oxide (blue).

Table S-1. Comparison of *l*, *w*, *i* and *s* (mm) for actual and mapped barcodes stamped on flat surfaces.

Parameter	Pattern Type	Rutile[a] on Anatase		Zinc oxide[b] on Anatase		Rutile on[c] anatase polyethylene wrap	
		A	B	A	B	A	B
l_1	Actual	9.5	9.5	10.0	10.0	9.6	9.6
	Map	10.5	10.5	9.6	9.6	9.5	9.5
l_2	Actual	9.4	9.4	8.8	8.8	9.2	9.2
	Map	9.8	9.8	8.8	8.8	9.0	9.0
l_3	Actual	9.5	9.5	10.8	10.8	-	-
	Map	9.8	9.8	10.8	10.8	-	-
w_1	Actual	0.3-0.4	0.3-0.4	0.3-0.6	0.3-0.6	0.4-0.5	0.4-0.5
	Map	0.5	0.5	0.3-0.6	0.3-0.6	0.3-0.6	0.3-0.6
w_2	Actual	0.3-0.4	0.3-0.4	0.2-0.4	0.2-0.4	0.4-0.5	0.4-.05
	Map	0.5	0.5	0.3-0.6	0.3-0.6	0.3-0.6	0.3-0.6
w_3	Actual	0.3-0.4	0.3-0.5	0.4-0.5	0.4-0.5	-	-
	Map	0.5	0.5	0.3-0.9	0.3-0.9	-	-
$i_{1\text{-}2}$	Actual	1.7-2.0	1.7-2.0	1.9	1.9	1.7-1.8	1.7-1.8
	Map	1.5-2.0	1.5-2.0	1.8	1.8	1.5-1.8	1.5-1.8
$i_{2\text{-}3}$	Actual	1.5-1.8	1.5-1.8	1.4-1.8	1.4-1.8	-	-
	Map	1.0-1.5	1.0-1.5	1.2-1.8	1.2-1.8	-	-
s_1	Actual	-	-	-	-	0.3	0.3
	Map	-	-	-	-	0.3	0.3
s_2	Actual	-	-	1.8	1.8	-	-
	Map	-	-	1.6	1.6	-	-
s_3	Actual	-	-	0.7	0.7	-	-
	Map	-		0.8	0.8	-	-

[a] $\theta_1 = \theta_2 = 20°$ for 120 seconds at each grid point; the 0.30 mm diameter collimator (d_{major} = 0.88 mm). [b] $\theta_1 = 60°$ and $\theta_2 = 5°$ for 120 seconds at each grid point; 0.30 mm diameter collimator (d_{major} = 0.35 mm). [c] $\theta_1 = 60°$ and $\theta_2 = 5°$ for 300 seconds at each grid point; 0.30 mm diameter collimator (d_{major} = 0.35 mm).

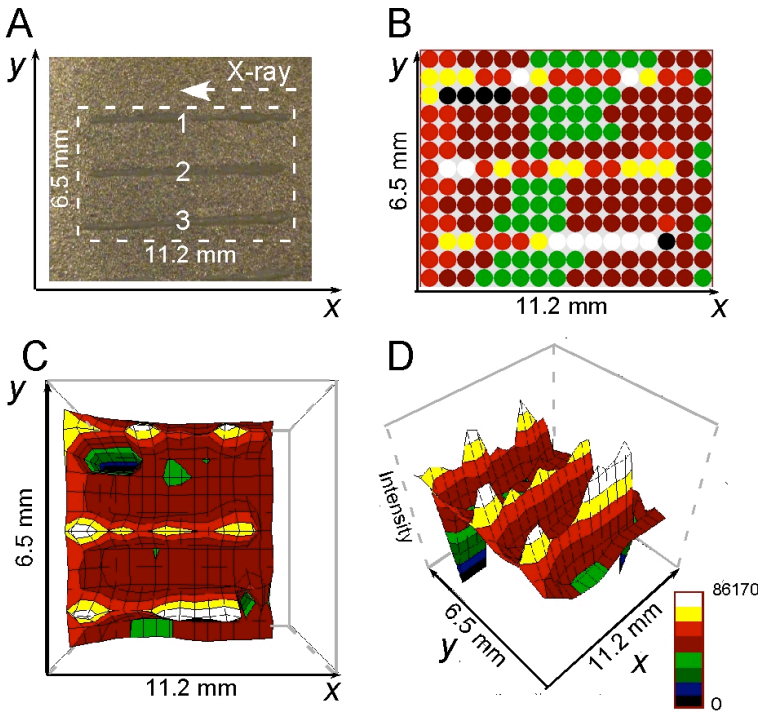

Figure S-2. Rutile barcodes on anatase films mapped with Method A. (A) Barcode of rutile stamped on an anatase film. The barcode consisted of 3 parallel bars (labeled 1, 2 and 3), with *l*, *w* and *i* values as reported in Table S-1. The rectangular mapping area is denoted by the dashed outline (X = 11.2 mm, Y = 6.5 mm). The grid point separations were Δx = 0.70 mm, Δy = 0.50 mm. (B) 2D μ-XRD plot. (C), (D) 3D μ-XRD plots acquired with Method A using the integrated area A_p for the (110) reflection at 2θ = 27.5°. Data were acquired at θ_1 = θ_2 = 20° for 120 seconds at each grid point using the 0.30 mm diameter collimator. The sample was aligned with the barcode lines parallel to the beam. The elliptical footprint of the beam has a major axis length d_{major} = 0.88 mm. The μ-XRD plots replicated the barcode (Table S-1). The total time required to map the entire grid was slightly less than seven hours.

Zinc oxide patterns on anatase films. μ-XRD mapping of a barcode of zinc oxide printed on a glass slide covered in anatase demonstrated that the protocol could be extended to other pattern materials that exhibits sufficient diffraction intensity for at least one (*hkl*) reflection. Using a barcode (Table S-1) different than the one described above for rutile, μ-XRD maps were acquired using either method A or B and the $(2\bar{1}\ 2)$ reflection at $2\theta = 68.0°$ (%crystallinity was measured over the range $67.5° \leq 2\theta \leq 68.6°$ for method B). The instrument settings were $\theta_1 = 60°$ and $\theta_2 = 5°$, and a rectangular mapping grid with dimensions X = 12.5 mm and Y = 5.9 mm with Δx = 0.40 mm and Δy = 0.30 mm and the 0.30 m diameter collimator were used (Figure S-3A).

The large θ_1 afforded a small footprint, d_{major} = 0.35 mm, which translates to the highest resolution attainable for this collimator. The total time required for mapping the barcode was 21 hours and 20 minutes. The μ-XRD maps were faithful replicas of the actual pattern (Table S-1, Figures S-3, S-4).

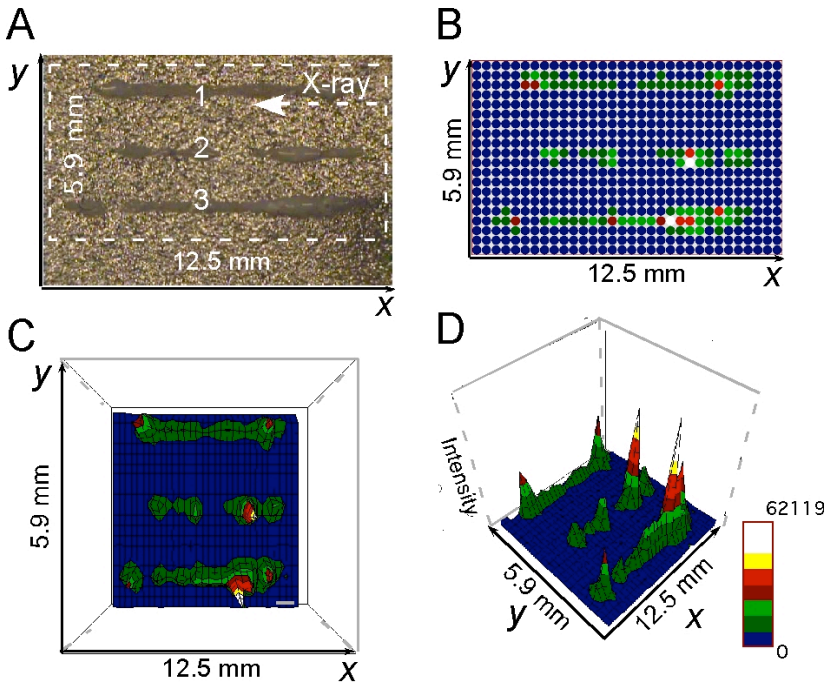

Figure S-3. Zinc oxide barcodes on anatase films mapped with Method A. (A) Barcode of zinc oxide stamped on an anatase film. The barcode consisted of 3 parallel bars (labeled 1, 2 and 3), with *l*, *w* , *i* and *s* values as reported in Table S-1. The rectangular mapping area is denoted by the dashed outline (X = 12.5 mm, Y = 5.9 mm). The grid point separations were Δx = 0.40 mm, Δy = 0.30 mm, (B) 2D μ-XRD plot. (C),(D) 3D μ-XRD plots acquired with Method A using the integrated area A_p for the (2-12) reflection at 2θ = 68.0°. Data were acquired at θ_1 = 60° and θ_2 = 5° for 120 seconds at each grid point using the 0.30 mm diameter collimator. The sample was aligned with the barcode lines parallel to the beam. The elliptical footprint of the beam has a major axis length d_{major} = 0.35 mm. The μ-XRD plots replicated the actual pattern (Table S-1). The total time required to map the entire grid was 21 hours and 20 minutes.

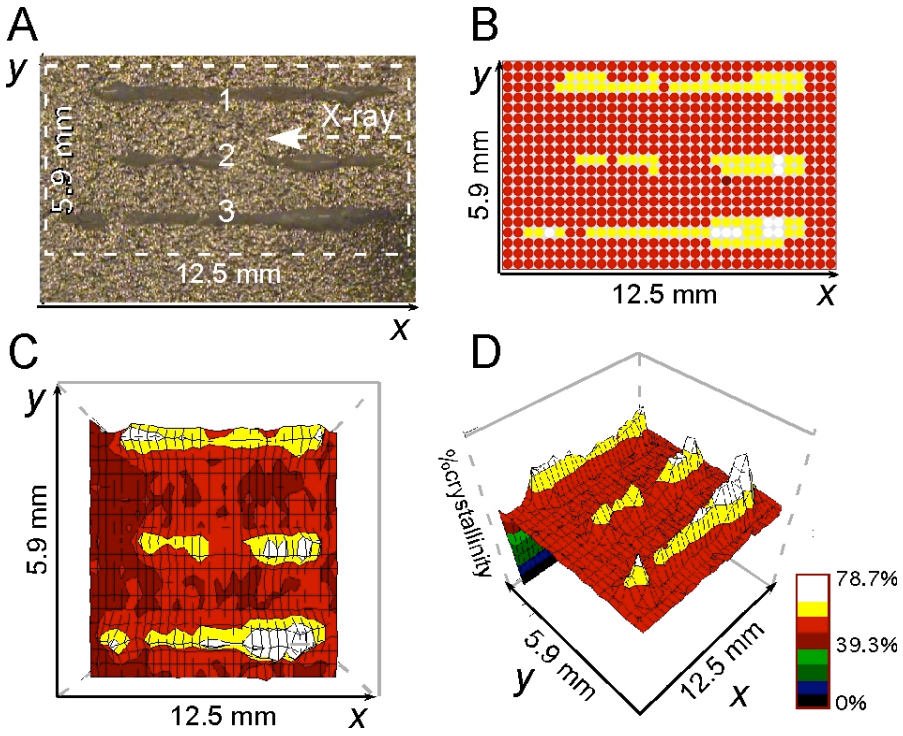

Figure S-4. Zinc oxide barcodes on anatase films mapped with Method B. (A) Barcode of zinc oxide stamped on an anatase film. The barcode consisted of 3 parallel bars (labeled 1, 2 and 3), with *l*, *w*, *i* and *s* values as reported in Table S-1. The rectangular mapping area is denoted by the dashed outline (X = 12.5 mm, Y = 5.9 mm). The grid point separations were Δx = 0.40 mm, Δy = 0.30 mm, (B) 2D μ-XRD plot. (C),(D) 3D μ-XRD plots of %crystallinity acquired with Method B across the range 67.5°≤ 2θ ≤ 68.6°. Data were acquired at θ_1 = 60° and θ_2 = 5° for 120 seconds at each grid point using the 0.30 mm diameter collimator. The sample was aligned with the barcode lines parallel to the beam. The elliptical footprint of the beam has a major axis length d_{major} = 0.35 mm. The μ-XRD plots replicated the actual pattern (Table S-1). The total time required to map the entire grid was 21 hours and 20 minutes.

Polyethylene film μ-XRD experiments. μ-XRD experiments were performed on corundum standard. The μ-XRD patterns were collected for 10 minutes at θ_1 = 60º and θ_2 = 20º with the sample covered with 6 layers of polyethylene film with thickness =15 μm (Figure S-5), and the intensities of the peak at 2θ = 76.9º were compared (Table S-2).

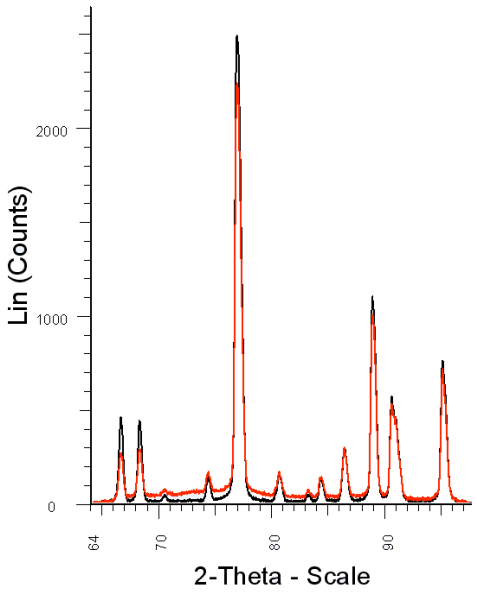

Figure S-5. Micro-XRD patterns of corundum (black) and corundum covered with 6 layers of polyethylene film with thickness = 15 μm (red) collected using the 0.50 mm collimator for 10 minutes at θ_1 = 60º and θ_2 = 20º.

Table S-2. Micro-XRD maximum intensities of the diffraction peak at 76.9º of corundum standard covered with layers of polyethylene film 15 μm thick collected at θ_1 = 60º and θ_2 = 20º for 10 minutes with the 0.50 mm collimator.

N[a]	Intensity[b] (Counts)	Intensity[b] (%)
0	2645	100
1	2624	99.2
2	2574	97.3
3	2544	96.2
4	2507	94.8
5	2447	92.5
6	2434	92.0

[a] Number of polyethylene layers 15 μm thick. [b] Maximum Intensity of corundum peak at 76.9º

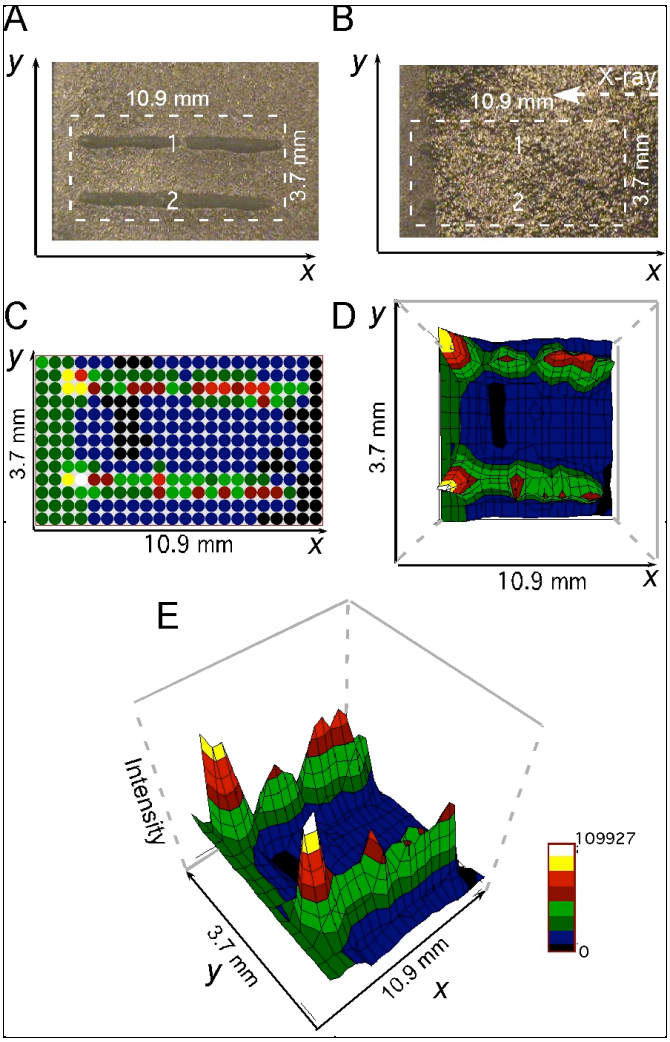

Figure S-6. Rutile barcodes on anatase films buried beneath polyethylene films, mapped with Method A. (A) Barcode of rutile stamped on an anatase film. The barcode consisted of 2 parallel bars (labeled 1 and 2), with *l*, *w* , *i* and *s* values as reported in Table S-1. The rectangular mapping area is denoted by the dashed outline (X = 10.9 mm, Y = 3.7 mm). The grid point separations were Δx = 0.50 mm, Δy = 0.30 mm. (B) The same sample covered with polyethylene wrap, (C) the 2-D μ-XRD plot. (D),(E) 3-D μ-XRD plots generated with Method A using the integrated area A_p for the (301) reflection at 2θ = 69.1°. Data were acquired at θ_1 = 60° and θ_2 = 5° for 300 seconds at each grid point using the 0.30 mm diameter collimator. The sample was aligned with the barcode lines parallel to the beam. The elliptical footprint of the beam has a major axis length d_{major} = 0.35 mm. The μ-XRD maps replicated the actual barcode (Table S-1). The total time required to map the entire grid was almost 24 hours.

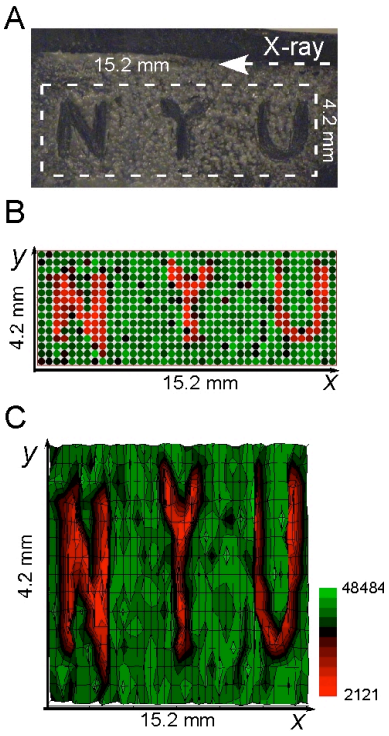

Figure S-7. Rutile logo on a silicon wafer mapped with Method B. (A) NYU logo of rutile stamped as a negative image on a silicon wafer. The rectangular mapping area is denoted by the dashed outline (X = 15.2 mm and Y = 4.2 mm). The grid point separations were Δx = 0.40 mm, Δy = 0.30 mm. (B) 2-D μ-XRD. (C) 3-D μ-XRD plots of %crystallinity acquired with Method B across the range 68.8°≤ 2θ ≤ 69.5°. Data were acquired at θ_1 = 60° and θ_2 = 5° for 180 seconds at each grid point using the 0.30 mm diameter collimator. The sample was aligned with the logo parallel to the beam. The elliptical footprint of the beam has a major axis length d_{major} = 0.35 mm. The logo was clearly legible in the μ-XRD plots. The total time required to map the entire grid was approximately 27 hours.

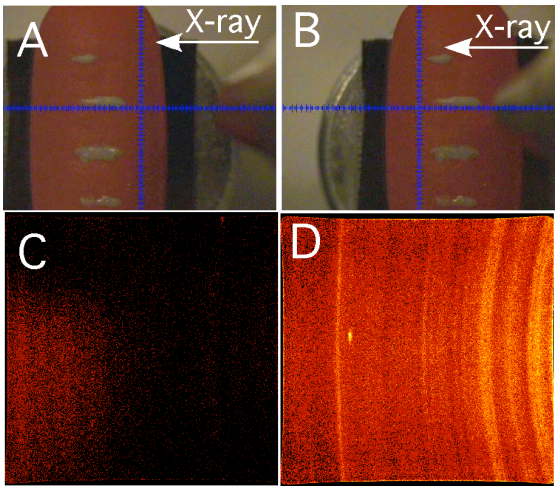

Figure S-8. (A) The scattering intensities of a point situated on the portion of a ibuprofen tablet near to the X-ray source is partially obscured from the tablet itself and unable to reach the detector. As a result, the μ-XRD pattern relative to that point of the tablet will exhibit lower intensity (C) than other points located to the opposite side of the tablet closer to the detector (B) and (D) affecting the outcome of the 2D and 3D μ-XRD plots. The white arrow depicts the X-ray direction.

Table S-3. Comparison of *l*, *w*, *i* and *s* parameters (mm) of actual and mapped barcodes printed on commercial ibuprofen and *aspirin tablets.

		Tablet 1[a]		Tablet 2[a]		Tablet $3_{(60°,=)}$[b]		Tablet $3_{(20°,=)}$[c]		Tablet $3_{(20°,\perp)}$[c]		*Tablet 4[f]	
		A[g]	B	A[g]	B	A	B	A	B	A[g]	B	A	B
l_1	Actual	4.0	4.0	5.7	5.7	1.0	1.0	1.0	1.0	1.0	1.0	5.0	5.0
	Map	-	4.0	-	7.0	-	0.9	-	0.9	-	1.0	5.1	4.2
l_2	Actual	-	-	5.5	5.5	1.8	1.8	1.8	1.8	1.8	1.8	6.6	6.6
	Map	-	-	-	5.6	1.8	1.8	-	1.8	-	1.5	6.0	6.0
l_3	Actual	-	-	-	-	2.2	2.2	2.2	2.2	2.2	2.2	-	-
	Map	-	-	-	-	2.1	1.8	1.2-1.8	1.8-2.4	-	2.5	-	-
l_4	Actual	-	-	-	-	2.2	2.2	2.2	2.2	2.2	2.2	-	-
	Map	-	-	-	-	2.1	2.1	1.8-2.1	2.1	-	2.5	-	-
l_5	Actual	-	-	-	-	1.2	1.2	1.2	1.2	1.2	1.2	-	-
	Map	-	-	-	-	1.2	1.2	0.9	1.2	-	1.0	-	-
i_{1-2}	Actual	-	-	1.2-1.5	1.2-1.5	1.6-1.7	1.6-1.7	1.6-1.7	1.6-1.7	1.6-1.7	1.6-1.7	1.5-1.8	1.5-1.8
	Map	-	-	-	1.5	-	1.8	-	1.2	-	1.5	1.5-1.8	1.5-1.8
i_{2-3}	Actual	-	-	-	-	1.5-1.6	1.5-1.6	1.5-1.6	1.5-1.6	1.5-1.6	1.5-1.6	-	-
	Map	-	-	-	-	1.5	1.5	-	0.9	1.5-1.8	1.5	-	-
l_{3-4}	Actual	-	-	-	-	1.7	1.7	1.7	1.7	1.7	1.7	-	-
	Map	-	-	-	-	1.8	1.8	1.5	0.9	-	1.5-2.0	-	-
l_{4-5}	Actual	-	-	-	-	1.5-1.6	1.5-1.6	1.5-1.6	1.5-1.6	1.5-1.6	1.5-1.6	-	-
	Map	-	-	-	-	1.5	1.8	1.2	0.9-1.2	-	1.5	-	-
w_1	Actual	0.3-0.5	0.3-0.5	0.5-0.7	0.5-0.7	0.3	0.3	0.3	0.3	0.3	0.3	0.4-0.7	0.4-0.7
	Map	-	0.5	-	0.5-1.0	-	0.3	-	0.6	-	0.5	0.3-0.6	0.3-0.6
w_2	Actual	-	-	0.2-0.7	0.2-0.7	0.4	0.4	0.4	0.4	0.4	0.4	0.4-0.7	0.4-0.7
	Map	-	-	-	0.5	0.6-0.9	0.6	-	1.2	-	0.5	0.3-0.6	0.3-0.6
w_3	Actual	-	-	-	-	0.7	0.7	0.7	0.7	0.7	0.7	-	-
	Map	-	-	-	-	0.3-0.6	0.3-0.6	0.9	1.2	-	0.5-1.0	-	-
w_4	Actual	-	-	-	-	0.5	0.5	0.5	0.5	0.5	0.5	-	-
	Map	-	-	-	-	0.3-0.6	0.3-0.6	0.9	0.6	-	0.5	-	-
w_5	Actual	-	-	-	-	0.4	0.4	0.4	0.4	0.4	0.4	-	-
	Map	-	-	-	-	0.3-0.6	0.3-0.6	0.6	0.6-0.9	-	0.5	-	-

μ-XRD maps acquired [a] at $\theta_1 = \theta_2 = 20°$ for 120 seconds at each grid point using the 0.5 mm diameter collimator (d_{major} = 1.5 mm), [b] at $\theta_1 = 60°$ and $\theta_2 = 5°$ for 200 seconds at each grid point using the 0.3 mm diameter collimator (d_{major} = 0.35 mm), [c] at $\theta_1 = \theta_2 = 20°$ for 120 seconds at each grid point using the 0.3 mm diameter collimator (d_{major} = 0.87 mm),) and [d] at $\theta_1 = 60°$ and $\theta_2 = 5°$ for 180 seconds at each grid point using the 0.3 mm diameter collimator (d_{major} = 0.35 mm). [g] The μ-XRD method did not reproduce the correct pattern.

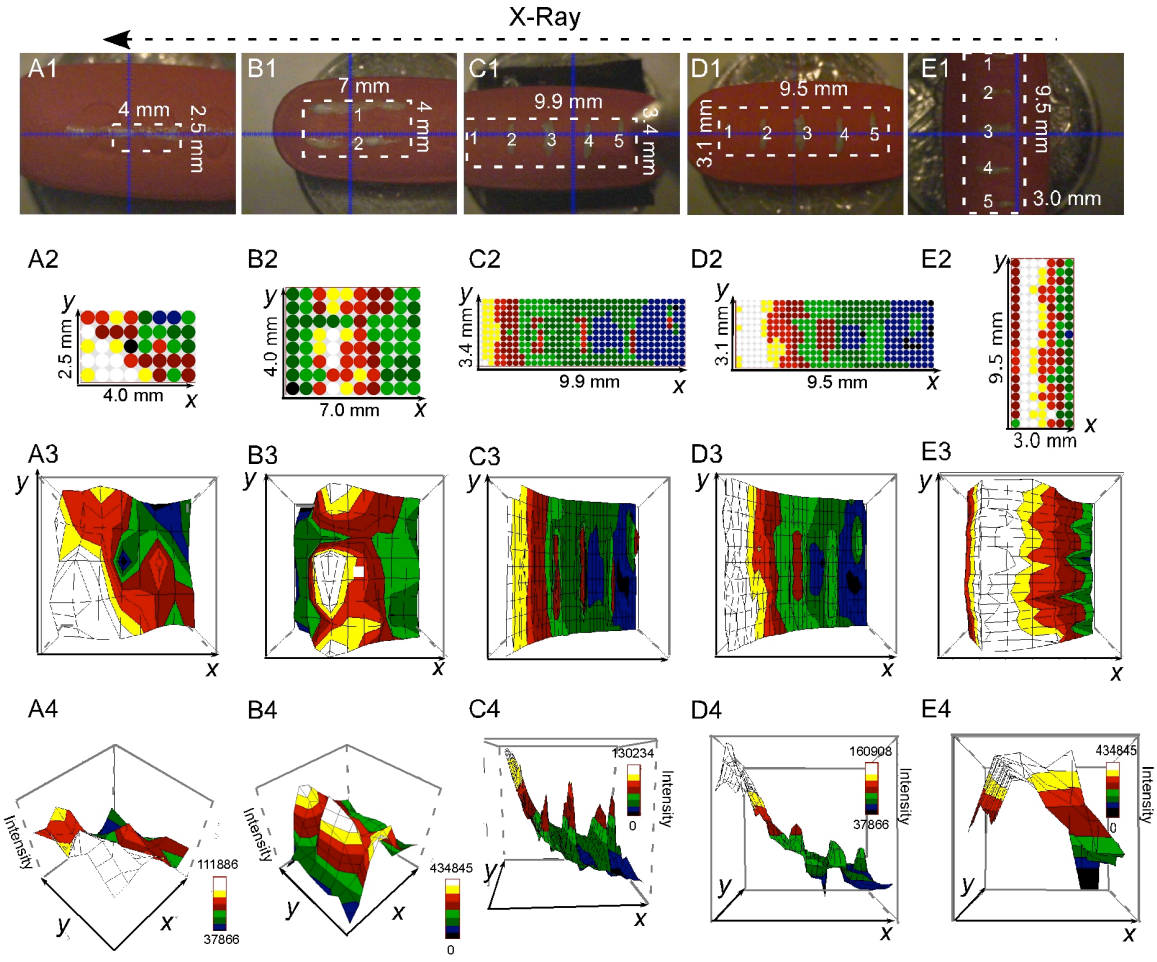

Figure S-9. Rutile barcodes on ibuprofen tablets mapped with Method A (see Table S-2 for *l*, *w* and *i* values) and the corresponding 2D and 3D μ-XRD plots acquired with Method A (see parameters in Table 2). The rectangular mapping areas are denoted by the dashed outlines. (A1-A4) Tablet 1; (B1-B4) Tablet 2; (C1-C4) Tablet 3 at *(60°,||)*; (D1-D4) Tablet 3 at *(20°,||)*; (E1-E4) Tablet 3 at *(20°,⊥)*. Data acquired at θ_1 = 60˚ afforded higher mapping resolution than θ_1 = 20˚ and smaller *w* values of the barcodes, but the lower θ_2 value of 5˚ required for the larger θ_1 resulted in greater X-ray absorption, increasing the baseline curvature of the 3D plots in (C4) compared with (D4). The absorption effect also increased with the curvature of the tablet (E4).

Barcodes on Aspirin Tablets. A μ-XRD map was acquired for a pattern stamped onto a commercial tablet of aspirin (Tablet 4) to evaluate the feasibility of the protocol on a differently shaped tablet. Tablet 4 (Figure S10) was stamped with a rutile barcode consisting of 2 lines (see Table S-3 for *l*, *w* and *i* values), and the μ-XRD mapping was performed using the parameters given in Table 2 and a rectangular mapping grid with X = 3.6 mm and Y = 6.9 mm, with Δx = 0.3 mm and Δy = 0.3 mm. The μ-XRD maps were

acquired with the 0.30 mm collimator using method A or B, the (301) reflection at 2θ = 69.1° (%crystallinity was measured over the range 68.8°≤ 2θ ≤ 69.5° for method B); θ_1 = 60°, θ_2 = 5° , scan area = 25 mm^2, and scan time = 180 sec per grid point. The sample was positioned with the barcodes perpendicular to the major axis of the elliptical footprint (d_{major} = 0.35 mm). The μ-XRD maps were faithful replicas of the actual pattern, although Method A proved superior (Figures S-10, S-11).

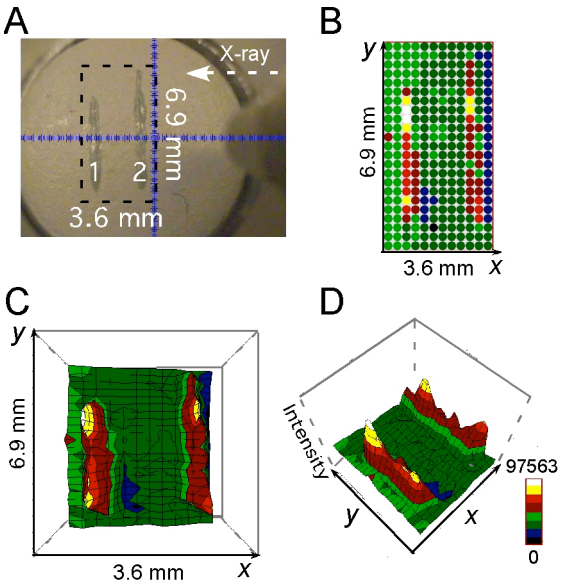

Figure S-10. Rutile barcode on a commercial aspirin tablet mapped with Method A. (A) Barcode of rutile (see Table S-2 for *l*, *w* and *i* values) on, (B) 2-D μ-XRD, (C) and (D) 3-D μ-XRD plots acquired with Method A using the parameters in Table 2. The black rectangle depicts the area mapped with the μ-XRD and the black arrow depicts the X-ray beam direction. The *x*-*y* axis and the color-scaled bars are also depicted. The aspirin tablets were biconvex and round with a diameter of 11.2 mm and a radius of curvature of 18.0 mm.

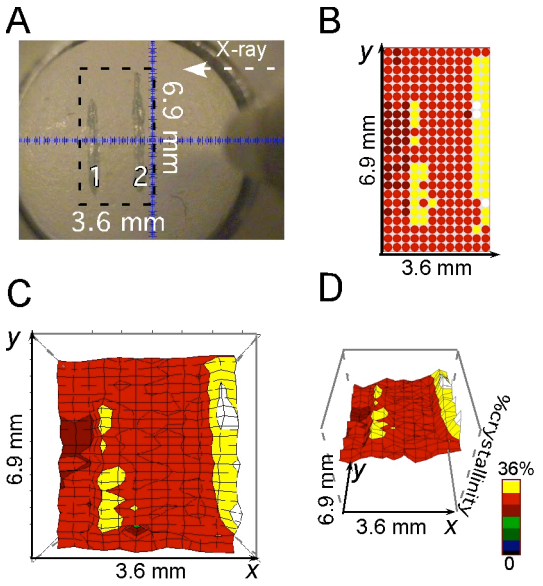

Figure S-11. Rutile barcode on a commercial aspirin tablet mapped with Method B. (A) Barcode of rutile (see Table S-3 for *l*, *w* and *i* values). (B) 2-D μ-XRD, (C) and (D) 3-D μ-XRD plots acquired with Method B using the parameters in Table 2. The black rectangle depicts the area mapped with the μ-XRD and the black arrow depicts the X-ray beam direction. The *x*-*y* axis and the color-scaled bars are also depicted. The aspirin tablets were biconvex and round with a diameter of 11.2 mm and a radius of curvature of 18.0 mm.

Micro-XRD experiments on ibuprofen and aspirin tablets. Micro-XRD experiments were performed on the external surface of ibuprofen and aspirin tablets, and micro-XRD patterns were collected for 180 seconds using the 0.30 mm diameter collimator at $\theta_1 = \theta_2 = 15°$ (Figure S-12). The tablets were cut in half, and micro-XRD patterns of the tablet cross-section were collected for 180 seconds using the 0.30 mm diameter collimator at $\theta_1 = \theta_2 = 15°$(Figure S-10).

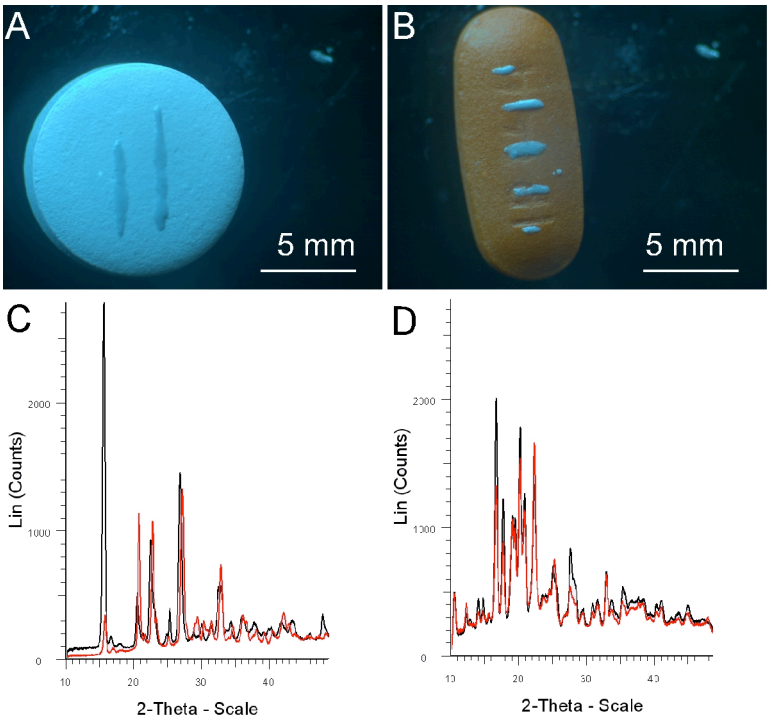

Figure S-12. Commercial (A) aspirin and (B) ibuprofen tablets used for micro-XRD mapping experiments. XRD patterns of the interior (red patterns) and exterior (black patterns) of (C) aspirin and (D) ibuprofen tablets collected at θ_1 = 60º and θ_2 = 5º for 180 seconds.